The optimal construction of a fiber-optic Fabry-Perot interferometer

Małgorzata Jędrzejewska-Szczerska*, Bogdan B. Kosmowski, Ryszard Hypszer

Faculty of Electronics, Telecommunications and Informatics,
Gdansk University of Technology, Narutowicza 11/12, 80-233 Gdańsk

Received June 15, 2009; accepted June 25, 2009; published June 30, 2009

Abstract— The authors present the optimization of fiber-optic Fabry-Perot interferometer design to attain the maximum resolution and accuracy of the sensor. The low-finesse Fabry-Perot interferometer working in reflective mode has been implemented. This interferometer was chosen for optimization because using it can have a lot of applications in practice. Its advantages are: a relatively simple configuration, potentially low cost, high resolution and low inertia on temperature changes. The authors present theoretical analysis and experimental results of optimization of the fiber-optic Fabry-Perot interferometer which has been designed and elaborated at our laboratory.

One of the commonly used interferometers is the Fabry-Perot interferometer, which fiber-optic arrangement (mirrors M_1 and M_2) is shown in figure 1.

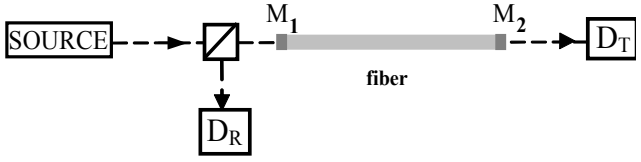

Fig.1. The fiber-optic, Fabry-Perot interferometer: M_1, M_2 – mirrors, D_R – detector in reflection mode, D_T – detector in transmission mode

This interferometer can work in the reflection or transmission mode. For the reflection mode, the amplitude of an electric vector of reflected light in the interferometer shown in Fig.1 is given [1]:

$$E_i = \frac{(1-e^{i\varphi})\sqrt{R}}{1-\mathrm{R}e^{i\varphi}} E_0 \qquad (1)$$

where: R – reflectivity of the mirror ($R=R_1=R_2$), φ – the phase difference between interfering beams, E_0 – the amplitude of an electric vector of an incident wave on the first mirror (M_1).

Exemplary constructions of such an interferometer as a fiber-optic device are shown in Figure 2. The interferometer shown in Figure 2.a is made as a thin film deposited on the end of the fiber. This Fabry-Perot interferometer has two boundary reflective surfaces: fiber/material and material/air [2]. The construction of the Fabry-Perot interferometer, shown in Figure 2.b, is made by the use of a capillary and a reflective plate (membrane). In case the capillary is filled by air, the reflective surfaces of this device are made by boundaries: fiber/air and air/reflective plate [3].

The interferometers shown in Figure 2 are low-finesse Fabry-Perot interferometers working in the reflective mode, which helps us to obtain a relatively high contrast. Taking this into account, amplitudes E_1 and E_2 of the waves reflected from the first and the second surface can be describe as follows:

$$E_1 = \sqrt{R_1}\, E_0$$
$$E_2 = (1-R_1)\sqrt{\alpha(x)R_2}\exp\left[-\frac{4\pi jnx}{\lambda}\right]E_0 \qquad (2)$$

where: E_1, E_2 – amplitude of the wave reflected from the surface of reflection coefficients - $R_1$and R_2, respectively; x – length of the Fabry-Perot cavity, n – refractive index of the Fabry-Perot cavity, $\alpha(x)$ – the attenuation coefficient of optical intensity due to the divergence of a light beam in the Fabry-Perot cavity.

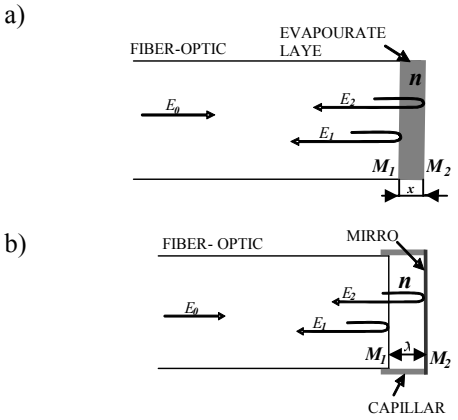

Fig.2. Constructions of fiber-optic Fabry-Perot interferometers: M_1, M_2 – surface with reflection coefficients, $R_1$and R_2 respectively; E_1,E_2 – amplitude of the wave reflected from surface M1, M2; x – length of the Fabry-Perot cavity; n – refractive index of the Fabry-Perot cavity

Optical intensity at the output of such an interferometer can be expressed by:

* E-mail: mjedrzej@eti.pg.gda.pl

$$I_{out} = \langle E\, E^{*} \rangle \tag{3}$$

where: $E = E_1+E_2$; the brackets $\langle\rangle$ – denote time averages; the asterisk $*$ – the complex conjugation.

By substituting from (2), equation (3) can be rewritten as [5]:

$$I_{out}(v) = I_c\left[1 + V_0 \cdot \cos\left(\Delta\varphi(v)\right)\right] \tag{4}$$

where:

$$I_c = I_0\left[R_1 + \left(1 - R_1\right)^2 \cdot R_2\alpha(x)\right] \tag{5}$$

$I_o = E_o^2$ – intensity of light incident on the first boundary surface of the interferometer, V_0 – visibility of the interference pattern in the spectral domain is expressed [4]:

$$V_0 = \frac{2\sqrt{\alpha(x)R_1R_2}\left(1-R_1\right)}{R_1 + \left(1-R_1\right)^2\alpha(x)R_2} \tag{6}$$

In order to attain the best metrological parameters in interferometric sensors the most important task is to maximize the visibility of the measured signal V_0.

It can be seen from that the maximization of the visibility value of the measured signal V_0 can be done by the optimal choice of the Fabry-Perot interferometer construction. A very important problem is to choose optical parameters of the material from which the cavity is made. The refractive index of the cavity material influences the value of the reflective coefficients of boundaries. Furthermore, theoretical investigation shows that one of the critical problems of the Fabry-Perot construction is the proper fitting of the geometrical dimension of the cavity because it influences the attenuation coefficient of optical signal intensity due to the divergence of a light beam in the Fabry-Perot cavity. Fiber-optic Fabry-Perot interferometers can be made with the use of multimode or single mode optic-fibers.

Using a simplified, geometrical model of rays propagation from multimode fiber into a interferometer cavity, attenuation $\alpha(x)$ of the intensity of an optical signal due to the beam divergence can be calculated. If the thickness of the Fabry-Perot cavity is x, $\alpha(x)$ is expressed as :

$$\alpha(x) = \frac{A^2}{\left[A + 2xtg(\sin^{-1}(NA))\right]^2} \tag{7}$$

where: A – the core radius, NA – the numerical aperture of the fibre.

Sensing the interferometer shown in Fig.2 can also be built using a single-mode fiber. It should be taken into consideration that the divergence of a light beam occurring at the end of a single-mode fiber is much higher than in a multimode fiber. This is caused by diffraction effects which are predominant in single-mode fibers. When the interferometer cavity length x is much larger than the diameter of the fiber core $2A$, only the first-order reflected beam from the end of the fibre and a small part of the first-order reflected beam from the surface will contribute to the interferometric signal. As the mode field diameter is approximated by the Gaussian profile, $\alpha(x)$ of an optical signal due to beam divergence can be calculated by using the equation [6]:

$$\alpha(x) = 1 - \exp\left[-\frac{2\omega_0^{\,2}}{\omega^2(x)}\right] \tag{8}$$

where: ω_0 – the mode field diameter, $\omega(x)$ – the mode field diameter at the x distance.

The authors of the present paper found out that visibility reaches its maximum value when:

$$R_2 = \frac{R_1}{\left(1-R_1\right)^2\alpha(x)} \tag{9}$$

It can be seen from equation (9) that in order to attain the maximum value of visibility, coefficient R_2 should have a very high value ($R_2 \approx 1$). Thus to define the value of R_1, which depends on the refractive index of the material of the interferometer cavity and the fiber, it is possible to estimate the optimal value of the interferometer cavity length.

To verify theoretical investigation an experimental set-up was designed and built. The system consists of a source, optical processor and the investigated Fabry-Perot interferometer. In low-coherent interferometery, which was used for experiments, it is possible to use the time domain or spectral domain signal processing.

When spectral signal processing is used, the measurement signal can be described as [7]:

$$I_{out}(\nu) = S(\nu)\left[1 + V_0\cos\left(\Delta\phi(v)\right)\right] \tag{8}$$

where: $S(v)$ - the spectral distribution of the light source; V_0 - visibility of interference fringes, $\Delta\phi\,(v)$ - the phase difference between interfering beams: $\Delta\phi(\nu) = 2\pi\ \nu\,\delta/c$, δ – optical path difference, c – velocity of the light in vacuum.

The authors employed the processing of optical measurement signals in the spectral domain, because of two important advantages. Firstly, such processing does not need any movable mechanical elements. Secondly, it is immune from any change in the optical transmission of the system. Measurement signal processing $S(v)$ is based on the channeled spectrum technique. When the extrinsic Fabry-Perot interferometer is illuminated by a low-coherent source, the reflection spectrum is modulated by the interference signal from the cavity. [8]

In the experimental set-up, superluminescent diodes with a Gaussian spectral density was used as a broadband source, (SLD type S1550-G-I-10 with central wavelength λ_0 = 1560 nm, $\Delta\lambda_{FWHM}$ = 45 nm, produced by SUPERLUM). An optical spectrum analyzer was implemented as an optical processor (Optical Spectrum Analyzer Ando AQ6319 with a wavelength resolution of 1 nm, wavelength accuracy of ±10 pm and a close-in dynamic range of 60 dB at peak ±100 pm). The low-finesse fiber-optic Fabry-Perot interferometer was applied as a sensing head, whose construction is shown in Figure 2b. Theoretical investigation showed that the use of monomode fiber should have been the most efficient. Hence, the investigated sensors were made from SM fiber, silicon capillary and a silver mirror. The interferometer consists of the fiber with an uncoated end which has the reflectance of 0,04. The second reflectance surface is made by a silver mirror with the reflectance of 0,99.Consequently, the authors got the system configuration solution close to optimum.

Figures 3.a and 3.b show the measured signal from the fiber-optic Fabry-Perot interferometer illuminated by a low coherent source.

In Figure 3a the measured signal form the low-coherent fiber-optic Fabry-Perot interferometer with an arbitrarily chosen length of interferometer cavity is shown. The signal from the interferometer with the optimal length of the interferometer cavity is presented in Figure 3.b.

It can be noted that the signal from the interferometer with the optimal construction has a bigger difference between the minimum (I_{min}) and maximum (I_{max}) values of the signal than that with random geometrical dimensions.

For the first interferometer with a measured signal shown in Figure 3a, the visibility is: V_0 = 0,67 and for the second, which measured signal is shown in Figure 3b, the visibility has the value: V_0 = 0,99.

These differences in visibility values confirmed that with the optimal selection of a geometrical dimension of the Fabry-Perot cavity it is possible to optimize its metrological parameters by improving the contrast of the measured signal.

The method of optimization of the fiber-optic, Fabry-Perot interferometer construction has been presented. The low-finesse Fabry-Perot interferometer working in the reflective mode has been investigated. This interferometer was chosen for optimization because of its broad range of potential applications. Its advantages are: relatively simple configuration, potentially low cost, high resolution and low thermal inertia. Furthermore, because of its small size it is possible to make nearly a point-wise measurement.

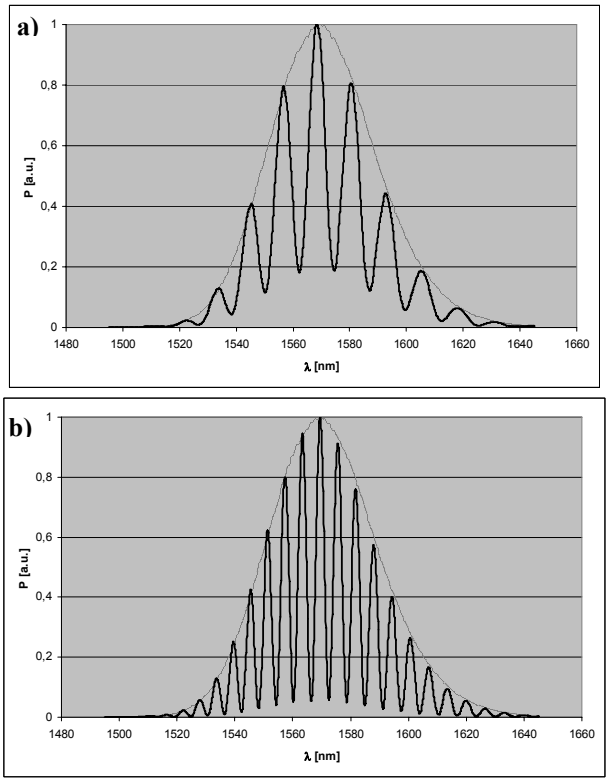

Fig.3. Measured signal from the low-coherent fiber-optic Fabry-Perot interferometer: a) with arbitrarily chosen the length of interferometer cavity; b) with the optimal length of interferometer cavity.

The use of multimode fiber and single-mode fiber in a Fabry-Perot sensor has been investigated theoretically and experimentally. A suitable construction was investigated in order to maximize fringe visibility.

The presented preliminary results can be the base for further work on building a fiber-optic sensor of physical quantities.

The current investigation is financed by the DS project of GUT Faculty of Electronics, Telecommunications and Informatics.

References

[1] T. Yoshino, K. Kurosawa, K. Itoh, and T. Ose, IEEE J. Quantum Electron. **18,** 1624 (1982)
[2] M. Jędrzejewska-Szczerska, R.Bogdanowicza, M.Gnyba, R.Hypszer, B.Kosmowski, Europ. Phys. Jour. ST **154**,107 (2008)
[3] F.Yu [ed]: *Fiber Optic Sensors* (New York, Marcel Dekker 2002)
[4] T.Liu, D.Brooks, A.Martin, R.Badcocko, G.Fernando, Proc. SPIE **2718**, 408 (1996)
[5] S.Egorov , A.Mamaev , I.Likhachiev, Proc. SPIE **2594**, 193 (1996)
[6] Bing Yu, Dae Woong Kim, Jiangdong Deng, Hai Xiao, Anbo Wang, Appl.Opt. **42**, 3241 (2003)
[7] S.Egorov, A.Mamaev, I.Likhachiev, Proc. of SPIE **1972**, 362 (1999)
[8] Shaoji Jiang, Bin Zeng, Youcheng Liang, Baojun Li, Opt. Eng. **46**, 034402-1÷5 (2007)

